CIRP Annals - Manufacturing Technology 00 (2020) 1–4

Contents lists available at ScienceDirect

CIRP Annals - Manufacturing Technology

journal homepage: https://www.editorialmanager.com/CIRP/default.aspx

Modal analysis of machine tools using visual vibrometry and output-only methods

Mohit Law[a,*], Pulkit Gupta[a], Suparno Mukhopadhyay[b]

[a] Machine Tool Dynamics Laboratory, Department of Mechanical Engineering, Indian Institute of Technology Kanpur, India
[b] Department of Civil Engineering, Indian Institute of Technology Kanpur, India

Submitted by Edvard Govekar (1), Ljubljana, Slovenia

ARTICLE INFO

Article history:
Available online xxx

Keywords:
Dynamics
Machine tool
Visual vibrometry

ABSTRACT

This paper presents visual vibrometry as a new video camera-based vibration measuring technique for machine tools. Pixels within images from recordings of the vibrating machine are treated as motion sensors to detect and track vibrating edges. Modal parameters are extracted from the measured pixel-displacement time series data using output-only mass-change methods. Methods are experimentally demonstrated on a small milling machine, on a slender boring bar, and on a regular end mill. Modal parameters extracted using visual vibrometry agree with those extracted using experimental modal analysis procedures. Moreover, visual vibrometry aids shape visualization and maintains advantages of other non-contact measurement techniques.

1. Introduction

Machine tool performance is governed by its dynamics. Knowledge of the dynamics helps in diagnostics, condition monitoring, structural design optimization, design of control strategies, and in the design of chatter-free machining strategies [1,2]. Hence, correctly measuring dynamics remains important.

Machine tool dynamics are usually measured using experimental modal analysis (EMA) procedures. EMA procedures involve using a load-cell instrumented modal hammer or shaker to excite the machine tool. Response is usually measured with contact type accelerometers and/or non-contact type laser Doppler vibrometers (LDV). Measured input-output time series data decomposed to the frequency domain results in frequency response functions (FRFs) that are processed to extract modal parameters, i.e., the natural frequencies, damping ratios, and mode shapes [3]. Though these methods have become routine, the added mass of the accelerometer may influence the measurements. It can also be sometimes difficult to decouple the interaction of the shaker with the machine. Moreover, experiments with expensive LDVs remain difficult to instrument. Furthermore, global shape analysis is tedious since it requires measurements at many discrete data points by roving the sensor or the actuator. Newer methods using 3D scanning LDVs and tracking interferometers [4], though quicker, are prohibitively expensive.

To address some of the above articulated challenges, this paper presents visual vibrometry as a new video camera-based vibration measuring technique for machine tools. By treating pixels within images from recordings of the vibrating machine as non-contact motion sensors, and by applying image processing techniques to detect and track vibrating edges, we extract the modal parameters of interest from the measured spatially dense full-field motion – which also makes shape analysis easier than other EMA methods.

Vision-based measurements also offer other advantages. Measurements need just a camera, a lens sometimes, and a computer with simple processing tools. Sophisticated data acquisition systems are also not required. For these reasons, vision-based measurements have found use across domains such as in transportation, experimental mechanics [5], material science [6], damage detection and non-destructive evaluation [7,8], modal testing of beams and cymbals [9–11], and in civil structural health monitoring of buildings, bridges, and cables [7,8,11].

In the context of machine tools, vision-based measurements have been used for tool condition monitoring and workpiece surface quality inspection [12,13]. Other exemplary work has used high-speed imaging techniques to study deformation mechanisms in machining [14,15] and to detect chatter [15]. However, machine tool modal parameter estimation using vision-based vibration measurements remains unreported yet.

The key technical contribution of this paper is to demonstrate the extraction of modal parameters of machine tools using vision-based measurements. Methods are illustrated with three examples. One example is that of a small milling machine, another is that of a slender boring bar mounted in a CNC lathe, and the third is that of an end mill mounted in a CNC milling machine. We impact the machine/tool to make it vibrate. All measurements are done for non-rotating tools and, for when machines are stationary. We use a high frame-rate camera to record high-frequency cutting tool vibrations and leverage the capabilities of modern smartphones to separately record lower-frequency tool and structural vibrations. Sampling in all cases respects the Nyquist criterion. Experimental setups and considerations are detailed in Section 2.

Detection and tracking the vibrating edge across images to obtain a sense of the motion is discussed in Section 3. Due to its robustness

* Corresponding author.
E-mail address: mlaw@iitk.ac.in (M. Law).

https://doi.org/10.1016/j.cirp.2020.04.043
0007-8506/

to image noise and ease of implementation, we prefer the Canny edge detector [16] over other or digital image correlation techniques [7,8], or optical flow-based schemes [9–11].

Extraction of modal parameters from the pixel-displacement time series data is discussed in Section 4. Since synchronizing sampling and triggering of camera recordings with the input force measurements is difficult, inputs are not measured, and modal parameters are estimated using output-only methods. We prefer the robust time-domain Eigensystem Realization Algorithm [17], although other modal identification methods may work as well [3,9]. Since the input was not measured, the eigenvector estimated was unscaled. And, since estimation of tool point FRFs requires mass-normalized eigenvectors, we propose a scheme based on the mass-change method [18] to correctly scale the eigenvector.

Modal parameters extracted from the vision-based measurements are benchmarked against results from the EMA approach in Section 5. The paper is concluded in Section 6.

2. Setups for video camera-based vibration measurements

Experimental setups to record videos are shown in Fig. 1. The small machine, the slender boring bar, and the end mill were excited using repeated impacts. Videos to record the resulting motion of the boring bar and the end mill were sampled at 5400 frames per second (fps) using a Photron FASTCAM SA 1.1 camera with a pixel resolution of 1024 × 1024. The camera was fitted with a 100 mm focal length lens. Distance between the lens and the tools was 100 mm. The field of view for the tools was 20 mm × 20 mm, resulting in 20 μm pixels. Motion of the boring bar was also separately recorded using a OnePlus 7 smartphone-based camera placed 200 mm away from the boring bar, sampling at 480 fps with a resolution of 720 × 1280 and a field of view of 36 mm × 64 mm, with a poorer per pixel resolution of 50 μm. Motion of the small machine was also recorded with the same phone camera sampling at 240 fps with a resolution of 1080 × 1920 and a field of view of 756 mm × 1344 mm, resulting in a poor per pixel resolution of 0.7 mm. Distance between the camera and the machine was 1 m.

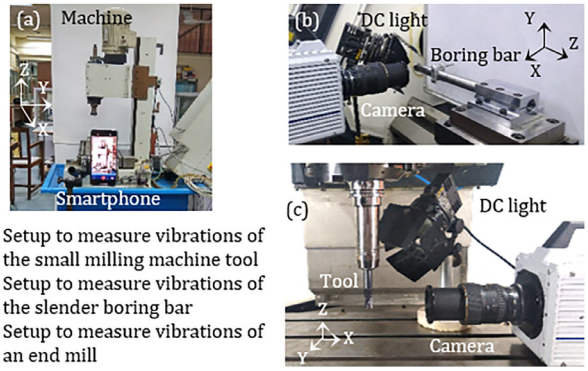

(a) Setup to measure vibrations of the small milling machine tool
(b) Setup to measure vibrations of the slender boring bar
(c) Setup to measure vibrations of an end mill

Fig. 1. Experimental setups for video camera-based measurements.

A DC light and a white background was used in all measurements to avoid flicker and ambiguities during edge detection. We do not use separate markers but use the objects' own features during detection. Since the displacement signal is only well defined at edges in the video and only in the direction perpendicular to the edges, only in-plane motion was measurable using a single camera setup shown in Fig. 1. Separate setups were hence necessary to record motion in different directions using the single camera.

Motion using the high-frame rate camera was captured for ~1 s, and each frame/image was saved in an uncompressed grayscale TIFF format using the Photron FASTCAM camera's software interface. Smartphone-based recordings lasted ~5 s. The smartphone's camera records videos in colour and in the MP4 format. Individual frames from these videos were read using the *VideoReader* function in MATLAB and converted to grayscale using the *rgb2gray* function. All images were further processed in MATLAB to extract displacements.

3. Extracting displacements by detecting and tracking edges

The edge of the vibrating object is first detected and then the same edge is tracked across successive frames to obtain a sense of its motion. An overview of this procedure is summarized in Fig. 2 for the representative case of the slender boring bar.

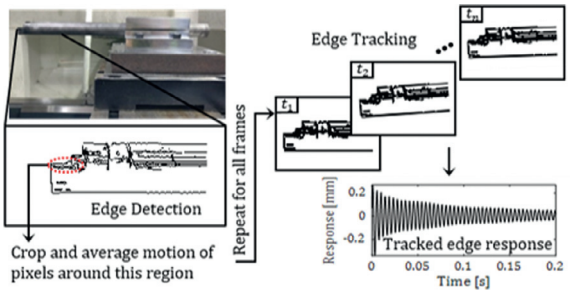

Fig. 2. Overview of the edge detection and tracking scheme.

We detect edges using the Canny edge detector [16], which we implement in MATLAB using the *edge* function. Detection involves finding pixels within images with sharp changes/discontinuities in their intensity gradients. This is preceded by convolving a Gaussian kernel/filter with the image to remove image noise. Edges are then marked at the maxima in gradient magnitude of a Gaussian-smoothed image.

All images were cropped to retain only the edge(s) of interest. The edge(s) of interest include the top edge of the boring bar, any of the side edges of the end mill, and all outer edges of the small milling machine. Cropped images retain between 100 and 300 pixels. Motion of these pixels is averaged for every frame, and the procedure is repeated for the next frame to finally result in the averaged pixel-displacement time series data.

4. Modal parameter extraction and FRF reconstruction

Natural frequencies, damping ratios, and unscaled mode shapes are extracted from the measured pixel-displacement time series data using the Eigensystem Realization Algorithm (ERA) [17]. The shapes are then scaled using mass-change methods [18].

4.1. Eigensystem realization algorithm for parameter extraction

An overview of main steps in the ERA is provided in Fig. 3. From the measured response, we first construct the Hankel matrix, $\mathbf{H}_0$. Next, we perform a singular value decomposition (svd) of $\mathbf{H}_0$ and select only the physical modes of the system by ordering the singular

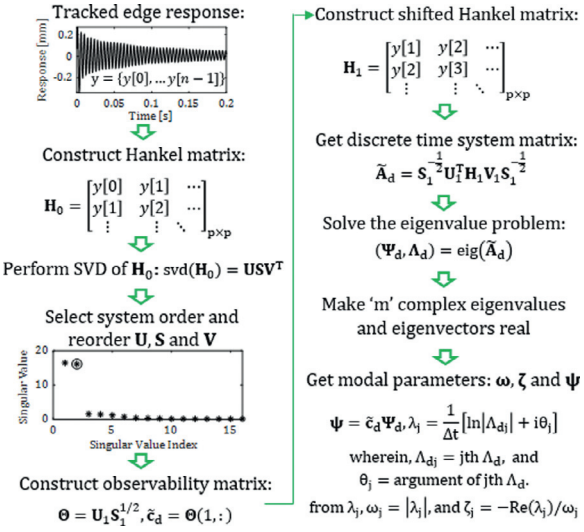

Fig. 3. Overview of the eigensystem realization algorithm.

Please cite this article as: M. Law et al., Modal analysis of machine tools using visual vibrometry and output-only methods, CIRP Annals - Manufacturing Technology (2020), https://doi.org/10.1016/j.cirp.2020.04.043

values. We then reorder the system matrices and construct a truncated observability matrix and a shifted Hankel matrix, $\mathbf{H}_1$. On obtaining the discrete system realization of the system matrix, $\tilde{\mathbf{A}}_d$, we obtain eigenvalues ($\mathbf{\Lambda}_d$) and eigenvectors (ψ_d) of $\tilde{\mathbf{A}}_d$. Conversion of the complex modes to real modes, and discrete time to continuous time, results in the natural frequencies (ω_j), damping ratios (ζ_j), and unscaled mode shapes (ψ_j).

4.2. Scaling eigenvectors using the mass-change method

Unscaled eigenvectors extracted from the ERA are scaled using the mass-change method [18] that requires additional visual vibrometry experiments with local changes in the mass distribution (Δm) of the tool(s) to cause a discernible change in the natural frequencies, and no perceptible change in the mode shapes of the mass-modified tool. Natural frequencies and unscaled eigenvectors of the original tool (ω_j, ψ_j) are used together with the natural frequencies and unscaled eigenvectors of the mass-modified tool ($\hat{\omega}_j, \hat{\psi}_j$) to obtain a scaling factor, α_j. An overview of this approach is shown in Fig. 4. Following recommendations in [18], a mass of ~42 g was placed at the anti-node (s) to result in a ~8% shift in ω_j and no discernable change in ψ_j.

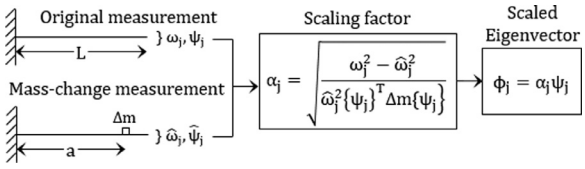

Fig. 4. Overview of procedure to correctly scale eigenvectors.

4.3. Reconstructing FRFs from extracted modal parameters

The tool point FRFs are reconstructed from the extracted modal parameters (ω_j, ζ_j, ϕ_j) for m modes of interest using:

$$h(\omega) = \sum_{j=1}^{m} \frac{\phi_j^2}{-\omega^2 + 2i\zeta_j\omega\omega_j + \omega_j^2}. \quad (1)$$

5. Experimental results

The visual vibrometry methods outlined above include estimating displacements by detecting and tracking the vibrating edge(s) of the structures of interest followed by modal parameter extraction using the ERA, followed by scaling of the shapes as required. Modal parameters extracted from the visual vibrometry (VV) methods are compared here with parameters obtained from the traditional experimental modal analysis (EMA) procedures. All measurements for EMA were processed using CutPRO®'s data acquisition and modal parameter extraction modules. We first discuss results for the small machine tool, followed by results for the boring bar, and then the end mill.

5.1. Visual vibrometry for a small machine tool

To demonstrate the ease with which full-field global mode shape analysis can be performed with VV, vibrations of the small machine tool were recorded with the smartphone camera by impacting the machine on its spindle. Since machine tool structural modes are typically of lower frequencies, the smartphone recording video at 240 fps is enough to capture the global modal behaviour. For the EMA method, a roving accelerometer was used to obtain response at 27 discrete locations by separately exciting the machine on the spindle for every measurement. Analysis discussed herein is limited to the machine's first global mode in the Y direction. As a first level analysis, the shape obtained using VV was left unscaled, and was magnified using motion magnification techniques [10] that involve band passing the video around the natural frequency to amplify motion for better visualization. The magnified shape is compared with the scaled shape obtained from EMA in Fig. 5– which also lists the extracted modal parameters. As is evident from the comparison in Fig. 5, the modal parameters and shape obtained with VV compare well with the EMA results.

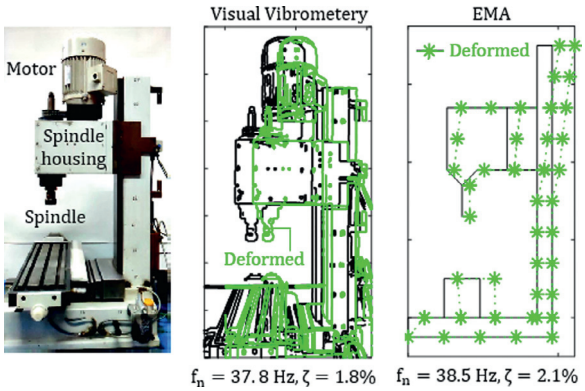

Fig. 5. Y-directional shapes and modal parameters of the small machine.

5.2. Visual vibrometry for a slender boring bar

The slender cantilevered boring bar that has a diameter of 25 mm, and a slenderness ratio of 12.5 was impacted at its free end, and its vibrations were measured with the high-frame rate camera as well as the smartphone camera. VV measurements were also conducted with and without the additional mass needed to scale the mode shapes. EMA was conducted using an instrumented modal hammer and a small single-axis piezoelectric accelerometer mounted on the tool tip. Tool point FRFs reconstructed with VV using the extracted modal parameters and correctly scaled shapes are compared with FRFs obtained using the EMA approach in Fig. 6. Analysis herein is limited to representative measurements only in the machine's Y direction.

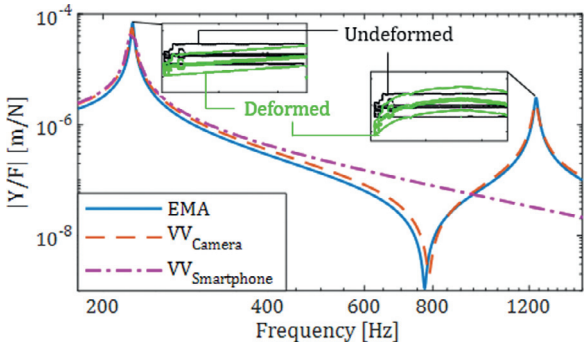

Fig. 6. Comparison of tool point FRFs of the slender boring bar.

As is evident from Fig. 6 and Table 1 that lists the extracted modal parameters, FRFs and parameters obtained with both methods compare well. Since the high-frame rate camera samples at 5400 fps, FRFs reconstructed using parameters identified from the camera-based response can faithfully capture the ~225 Hz low-frequency mode as well as ~1235 Hz higher-frequency mode. However, since the smartphone camera samples at 480 fps it cannot measure the ~1235 Hz high-frequency tool mode.

Table 1
Comparison of modal parameters for the slender boring bar.

	Visual Vibrometry			EMA		
	ω_n [rad/s]	ζ [%]	ϕ	ω_n [rad/s]	ζ [%]	ϕ
1st mode	$2\pi \cdot 225.9$	0.77	1.32	$2\pi \cdot 226.5$	0.50	1.19
2nd mode	$2\pi \cdot 1232.1$	0.94	1.65	$2\pi \cdot 1235$	0.65	1.55

Please cite this article as: M. Law et al., Modal analysis of machine tools using visual vibrometry and output-only methods, CIRP Annals - Manufacturing Technology (2020), https://doi.org/10.1016/j.cirp.2020.04.043

Since the smartphone-based measurements cannot estimate the higher-frequency mode, Table 1 lists only the modal parameters extracted from the high-frame rate camera-based measurements. As is evident, though the natural frequencies compare very well, damping ratios and scaled eigenvectors estimated using VV are slightly higher than those estimated by the EMA procedures.

Visual vibrometry also facilitates the easy evaluation of mode shapes, and Fig. 6 shows the shapes associated with each mode which were obtained using separate far-field VV experiments. These shapes were scaled using motion magnification techniques to aid visualization [10]. The low-frequency mode is the classical first bending mode of a cantilevered tool, and the higher-frequency shape corresponds to the second bending mode. This example also demonstrates how the VV method can effectively estimate modal parameters for systems with multiple modes.

5.3. Visual vibrometry for a milling tool

Vibrations of a 16 mm diameter end mill held in a hydraulic expansion toolholder mounted in a milling spindle with an overhang of 225 mm from the spindle nose were recorded with the high-frame rate camera. Separate VV and EMA setups were necessary to measure dynamics in the X and Y directions. In both cases the tool tip was excited using impacts, which were measured for EMA, and remained unmeasured for VV. For EMA measurements, the response was measured with a small accelerometer mounted on the tool tip. VV measurements were also conducted with and without the additional mass needed to correctly scale the eigenvectors. Tool point FRFs were reconstructed using the extracted modal parameters using two separate methods for the two different measurement techniques. Reconstructed FRFs are compared in Fig. 7. End mill dynamics had only a single dominant mode in the X and Y directions in the frequency range of interest, i.e., from 20 – 3000 Hz. Extracted modal parameters are listed and compared in Table 2.

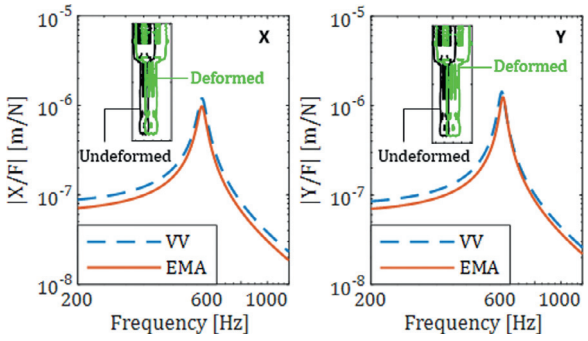

Fig. 7. Comparison of X and Y directional tool point FRFs for the endmill.

Table 2
Comparison of X and Y directional modal parameters for the end mill.

	Visual Vibrometry			EMA		
	ω_n [rad/s]	ζ [%]	ϕ	ω_n [rad/s]	ζ [%]	ϕ
X	$2\pi \cdot 574.6$	3.24	1.01	$2\pi \cdot 574$	3.20	0.90
Y	$2\pi \cdot 606.2$	2.64	1.05	$2\pi \cdot 612$	2.50	0.96

As is evident from Fig. 7 and Table 2, the modal parameters and the FRFs are in very close agreement. The peak amplitudes of the FRFs reconstructed with the VV approach are slightly higher than the results obtained with EMA due to the eigenvectors estimated with VV being slightly higher. The damping ratios compare rather well, and there are negligible differences in the natural frequency estimates using both methods. Fig. 7 also shows the associated mode shapes for the X and Y directional modes. As was done for the small milling machine example, and for the slender boring bar, separate far-field visual vibrometry experiments were performed on the end mill and motion magnification techniques [10] were adopted to aid visualization of the tool deflection shapes. The shapes make clear the combined bending motion of the tool and the tool holder in different directions. Such shape analysis is simpler with the VV approach than it is with the EMA approach.

6. Conclusions

This paper introduced a new method to extract machine tool modal parameters to reconstruct tool point FRFs using vision-based vibration measurements. A high-frame rate camera and a smartphone camera were used to record videos of a vibrating milling machine, a slender boring bar, and an end mill. Motion was detected and tracked using image processing techniques. Modal parameters were identified using output-only mass-change methods, and were found to agree with the parameters extracted from the traditional experimental modal analysis (EMA) methods. Mode shape analysis was shown to be much simpler using visual vibrometry methods than it is with EMA methods.

Visual vibrometry using output-only mass-change methods necessitate additional measurements to correctly scale the eigenvector. This can be avoided by synchronizing sampling and triggering of the camera recordings with the input – which needs to be addressed systematically. Furthermore, addressing potential uncertainties in edge detection and tracking is also warranted.

Acknowledgements

The Authors acknowledge partial support from the Government of India's IMPRINT initiative through project number 5509, and the High-speed Experimental Stress Analysis Lab at the IIT Kanpur for access to its high frame rate camera for measurements.

References

[1] Okubo N, Yoshida Y (1982) Application of Modal Analysis to Machine Tool Structures. *CIRP Annals* 31(1):243–246.
[2] Munoa J, et al. Chatter Suppression Techniques in Metal Cutting. *CIRP Annals* 65 (2):785–808.
[3] Ewins DJ (2000) *Modal Testing: Theory, Practice, and Application*, Research Studies Press LtdBaldock, Hertfordshire, England.
[4] Brecher C, et al. Experimental Modal Analysis Using a Tracking Interferometer. *CIRP Annals* 63(1):345–348.
[5] Sutton M A, et al. (2009) *Image Correlation for Shape, Motion, and Deformation Measurements: Basic Concepts, Theory and Applications*, SpringerLink, Boston, MA, USA.
[6] Davis A, et al. (2017) Visual Vibrometry: Estimating Material Properties from Small Motions in Video. *IEEE Transactions on Pattern Analysis and Machine Intelligence* 39(4):732–745.
[7] Feng D, Feng M (2018) Computer Vision for SHM of Civil infRastructure: From Dynamic Response Measurement to Damage Detection – A Review. *Engineering Structures* 156:105–117.
[8] Spencer Jr. BF, Hoskere V, Narazaki Y (2019) Advances in Computer Vision-Based Civil Infrastructure Inspection and Monitoring. *Engineering* 5(2):199–222.
[9] Javh J, et al. The Subpixel Resolution of Optical-Flow-Based Modal Analysis. *Mechanical Systems and Signal Processing* 88:89–99.
[10] Chen J, et al. Modal Identification of Simple Structures with High-Speed Video Using Motion Magnification. *Journal of Sound and Vibration* 345:58–71.
[11] Xu Y, Brownjohn JMW (2018) Review of Machine-Vision Based Methodologies for Displacement Measurement in Civil Structures. *Journal of Civil SHM* 8(1):91–110.
[12] Kurada S, Bradley C (1997) A Review of Machine Vision Sensors for Tool Condition Monitoring. *Computers in Industry* 34(1):55–72.
[13] Dutta S, et al. Application of Digital Image Processing in Tool Condition Monitoring: A Review. *CIRP Journal of Manufacturing Science and Technology* 6 (3):212–232.
[14] Guo Y, et al. In Situ Analysis of Flow Dynamics and Deformation Fields in Cutting and Sliding of Metals. *Proceedings of the Royal Society A* 471:20150194.
[15] Berezvai S, et al. High-Speed Camera Measurements in the Mechanical Analysis of Machining. *Procedia CIRP* 77:155–158.
[16] Canny J (1986) A Computational Approach to Edge Detection. *IEEE Transactions on Pattern Analysis and Machine Intelligence* 8(6):679–698.
[17] Juang J, Pappa R (1985) An Eigensystem Realization Algorithm for Modal Parameter Identification and Model Reduction. *Journal of Guidance, Control, and Dynamics* 8:620–627.
[18] López-Aenlle M, et al. Scaling-Factor Estimation Using an Optimized Mass-Change Strategy. *Mechanical Systems and Signal Processing* 24(5):1260–1273.